



Providing Choice & Value

Generic CT and MRI Contrast Agents



**FRESENIUS
KABI**

CONTACT REP

AJNR

**Comparison of Fluid-attenuated
Inversion-recovery MR Imaging with CT in a
Simulated Model of Acute Subarachnoid
Hemorrhage**

Kyo Noguchi, Hikaru Seto, Yuichi Kamisaki, Gakuto Tomizawa,
Shinichiro Toyoshima and Naoto Watanabe

This information is current as
of July 25, 2025.

AJNR Am J Neuroradiol 2000, 21 (5) 923-927
<http://www.ajnr.org/content/21/5/923>

Comparison of Fluid-attenuated Inversion-recovery MR Imaging with CT in a Simulated Model of Acute Subarachnoid Hemorrhage

Kyo Noguchi, Hikaru Seto, Yuichi Kamisaki, Gakuto Tomizawa, Shinichiro Toyoshima, and Naoto Watanabe

BACKGROUND AND PURPOSE: Because MR imaging is becoming integral to the evaluation and treatment of very early stroke, it is critical to prove that MR imaging is at least as sensitive to acute subarachnoid hemorrhage (SAH) as is CT. The present study was conducted to evaluate the possibility of detecting a small amount of acute SAH diluted by CSF not revealed by CT but identified on fluid-attenuated inversion-recovery (FLAIR) MR images in an in vitro study.

METHODS: Acute SAH was simulated with mixtures of artificial CSF and arterial blood (hematocrit [Hct], 45%) ranging from 0% to 100% by volume. We scanned these phantoms with CT and turbo-FLAIR MR imaging (9000/119 [TR/effective TE]; inversion time, 2200 ms; echo train length, 7), and we measured T1 and T2 relaxation times of these phantoms at temperatures within 36° C to 37° C. Plots of CT value from the different blood/water mixture ratios versus Hct were generated and correlated with the average CT value from normal cortex. We measured T1 and T2 relaxation times of these phantoms and normal cortex and generated T2 relaxation curves as a function of effective TE for a specific inversion time (2200), and determined the TR (9000) for the turbo-FLAIR sequence by using a theoretical equation for the turbo inversion recovery signal intensity.

RESULTS: Above a Hct of 27% blood, the mixture was denser on CT scans than was the normal cortex. At a selected time longer than an effective TE of 120, above a Hct of 22.4% blood, the mixture was more hyperintense than the normal cortex on turbo-FLAIR images. At selected times longer than an effective TE of 160, above a Hct of 9% blood, the mixture was more hyperintense than was the normal cortex.

CONCLUSION: FLAIR imaging is more sensitive than CT in the detection of a small amount of acute SAH diluted by CSF at selected appropriate TE, as determined in an in vitro study.

CT is central to assessing acute subarachnoid hemorrhage (SAH) and has generally replaced lumbar puncture for this purpose (1). CT scanning, however, is unreliable for detecting subarachnoid blood produced by a minor leak (2, 3). If the minor leak is unrecognized and a subsequent major rupture occurs, the SAH is more severe, and the clinical condition of the patient becomes more precarious.

Emergency evaluation of acute stroke must be conducted very quickly. Because MR imaging is becoming integral to the evaluation and treatment of very early infarction, it is critical to prove that MR imaging is at least as sensitive to acute SAH as CT is. It is generally accepted, however, that acute SAH is difficult to detect with conventional MR imaging (4–6). Several recent studies have reported that fluid-attenuated inversion-recovery (FLAIR) or turbo-FLAIR imaging reliably provides diagnostic images of acute or subacute SAH (7–11).

The present study was conducted to evaluate the possibility of detecting a small amount of acute SAH diluted by CSF not revealed by CT with FLAIR imaging in an in vitro study. If minor leaks are not revealed by CT, but are diagnosed after using FLAIR or turbo-FLAIR imaging before a major rupture, it is likely that future stroke evaluation will

Received September 17, 1999; accepted after revision November 24.

From the Department of Radiology, Toyama Medical and Pharmaceutical University, Toyama, Japan.

Supported in part by a Grant-in-Aid for Encouragement of Young Scientists.

Address reprint requests to Kyo Noguchi, MD, Department of Radiology, Toyama Medical and Pharmaceutical University, 2630 Sugitani, Toyama City, 930-0194, Toyama, Japan.

© American Society of Neuroradiology

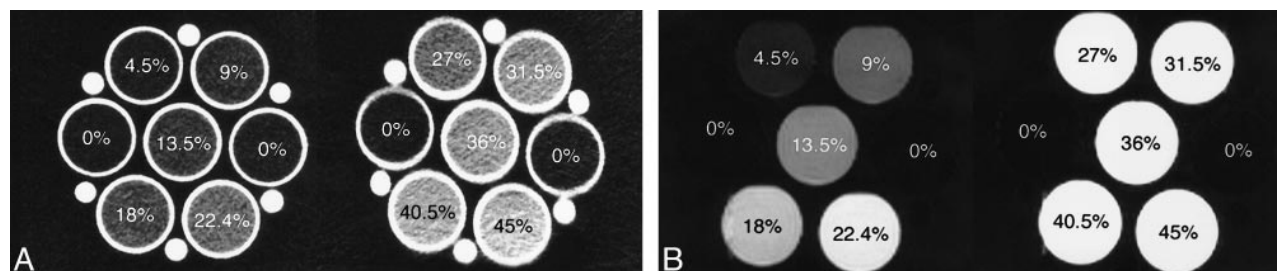


FIG 1. CSF (Hct, 0%) and each simulated SAH (ranging from Hct 4.5% to 45%).

A, CT scan.

B, Turbo-FLAIR image (9000/119 [TR/effective TE]; inversion time, 2200 ms).

be performed entirely by MR imaging rather than by CT.

Methods

Phantom Study

Volume mixtures of arterial blood (hematocrit [Hct], 45%; hemoglobin, 14.8 mg/dL) from healthy volunteers and artificial CSF ranged from 0% blood (100% water) to 100% blood (whole blood) (Fig 1). The artificial CSF was prepared according to the method described by Oka et al (12). Heparinization of the blood was performed to maintain it in solution. Eleven different solutions were generated and placed in standard plastic syringes (diameter, 2.5 cm; volume, 30 mL), and these plastic syringes were placed in a larger plastic syringe filled with normal saline (17-cm cube; volume, approximately 4900 mL). The larger syringe was wrapped in towels to maintain the phantom temperature.

Preliminary results indicated that, if the routine turbo-FLAIR parameters (inversion time, 2200 ms; TR, 9000 ms) were used, with pure phantom water at room temperature (approximately 24°C), signal intensity was not nulled. We attributed this to the fact that T1 relaxation time of water is temperature-dependent (13, 14) (ie, the null point of the water is temperature-dependent). Therefore, these phantoms were heated and maintained at 37°C and were scanned with CT and turbo-FLAIR imaging. The T1 and T2 relaxation times of these phantoms were measured at temperatures within 36°C to 37°C.

MR imaging was performed on a 1.5-T superconducting unit. MR images of the phantom were obtained with a standard head coil. The turbo-FLAIR examination was performed at 9000/119 (TR/effective TE), with a TI of 2200 ms and an echo train length of 7. Six multiple spin-echo images with TRs equal to 250, 500, 750, 1000, 2000, and 3000 and a TE of 14 were acquired for the T1 relaxation time calculations. Images used for T2 relaxation time calculations were acquired using the Carr-Purcell spin-echo technique (TR, 5000; 16 multiple TE, ≤ 800). Instrumental parameters included a 23-cm field of view, a 144 × 256 matrix, and a 10-mm section thickness. One excitation was acquired.

Turbo-FLAIR signal intensity measurements and T1 or T2 relaxation time calculations were made from circular regions of interest (ROI) with a fixed 1.5-cm diameter. These relaxation time calculations were performed using standard software.

CT examinations were performed at 10-mm section thickness in the phantom study, using a 900S scanner. The interval between the linked CT and MR examinations was less than 3 hours. CT values (Hounsfield units [HU]) were made from circular ROI with a fixed 1.5-cm diameter.

Human Study

T1 and T2 measurements were obtained from the eight healthy volunteers (age range, 26–65 years; average age, 52

years). ROIs (1.5-cm diameter circle) were placed in the cortical gray matter (including white matter) locations, and T1 and T2 measurements were obtained from those regions. CT values (in HU) were obtained from the 24 healthy volunteers (age range, 32–75 years; average age, 55 years). ROIs (1.5-cm diameter circle) were placed in the cortical gray matter (including white matter) locations, and the CT value in these regions was measured.

Graph Analysis

Plots of simulated SAH/CSF ratio (ie, the density or signal intensity of the bloody CSF divided by the density or signal intensity of normal CSF) from CT scans and turbo-FLAIR images versus Hct were generated. Plots of CT value (in HU) versus Hct were generated and correlated with the average CT value from the normal cortical gray matter. The T1 and T2 relaxation times of the phantoms and the normal cortical gray matter were used for generating T2 relaxation curves as a function of effective TE for a specific inversion time (2200). TR (9000) was obtained in the turbo-FLAIR sequence by using a theoretical equation for turbo inversion recovery signal intensity (15).

Results

The SAH/CSF ratio of the turbo-FLAIR images radically increased with an increase in Hct, reaching the highest SAH/CSF ratio above a Hct of 40.5% blood. The SAH/CSF ratio of the turbo-FLAIR images versus Hct had a nonlinear relation; in contrast, the SAH/CSF ratio of the CT versus Hct had a linear relation (Fig 2).

The CT value gradually increased with an increase in Hct. CT value versus Hct had a linear relation (Fig 3). The highest CT value was measured at Hct 45% (whole blood) (55 HU) and the lowest was at 2.4 HU for artificial CSF. Above a Hct of 27% blood, the mixture was denser on CT scans than normal cortical gray matter was (average, 34 HU).

The T1 and T2 relaxation times of the mixtures decreased with increasing blood Hct, ranging from 2860 to 1284 ms (T1 time) and from 1985 to 153 ms (T2 time). Figure 4 illustrates the T2 relaxation curves of normal cortical gray matter, CSF, and each simulated SAH as a function of effective TE for a specific inversion time (2200) and TR (9000) in a turbo-FLAIR sequence by using a theoretical equation for turbo-inversion recovery signal intensity. The signal of artificial CSF was reduced in the

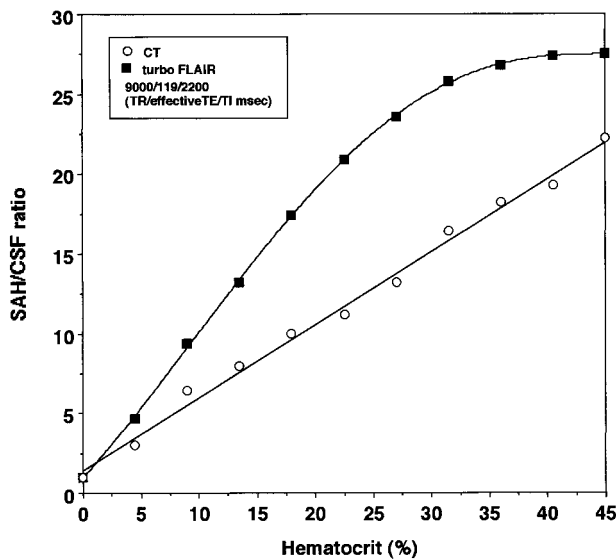


FIG 2. Plots of simulated SAH:CSF ratio versus Hct (%).

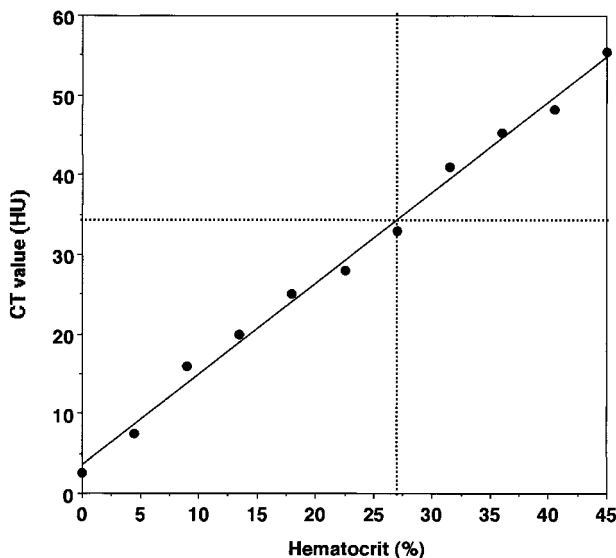


FIG 3. Plots of CT value (in HU) versus Hct (%) and correlation with the average CT value of the normal cortical gray matter.

turbo-FLAIR T2 relaxation curves. At selected times longer than an effective TE of 120, above a Hct of 22.4% blood, the mixture was more hyperintense than was the normal cortical gray matter on turbo-FLAIR images. At selected times longer than an effective TE of 160, above a Hct of 9% blood, the mixture was more hyperintense than was the normal cortical gray matter.

Discussion

The diagnosis of acute SAH with CT scanning is highly regarded in clinical practice (1, 16, 17). CT scanning, however, is unreliable for revealing the subarachnoid blood produced by a small bleed (2, 3). The depiction of SAH with CT depends on the attenuation values of the blood in the CSF spaces, whereas that of MR imaging mainly depends on

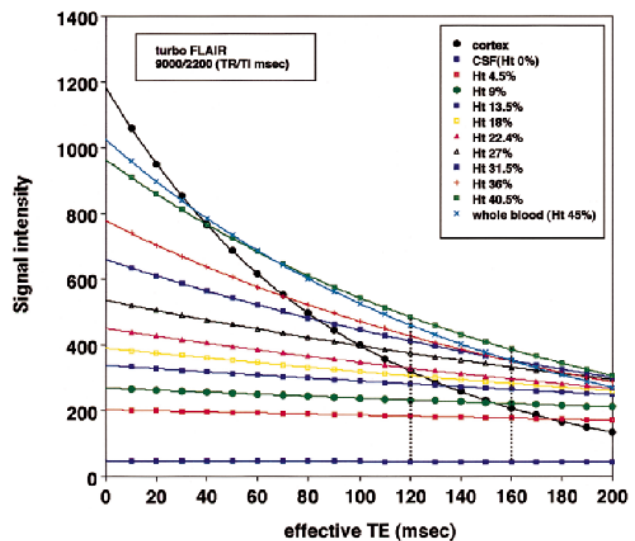


FIG 4. T2 relaxation curves of normal cortical gray matter, CSF (Hct, 0%), and each simulated SAH (ranging from Hct 4.5% to 45%) as a function of effective TE for a specific inversion time (2200 ms) and TR (9000) in a turbo-FLAIR sequence by using a theoretical equation for turbo inversion recovery signal intensity.

the difference of the T1 and T2 relaxation times of the SAH relative to those of the CSF and brain parenchyma.

Chakeres and Bryan (18) postulated that MR imaging may be superior to CT for the detection of SAH based on their in vitro data for CSF-blood mixtures at lower CSF/blood ratios. Nevertheless, it is generally accepted that acute SAH is difficult to detect with conventional MR imaging (4–6). Recently, it was reported that acute SAH could be clearly shown as an area of high signal intensity on FLAIR images and that FLAIR imaging is comparable with CT in the detection of acute SAH (7, 8, 10, 11). In addition, these reports have shown that, in many cases, the extent of the abnormality was clearly more extensive on the FLAIR images than on the CT scans (7, 8, 10, 11).

The CT attenuation value of blood is related linearly to Hct and hemoglobin (17). Although CSF protein concentration also shows a linear relationship with the CT attenuation value, the normal and pathologic ranges show only a minimal change (17). Therefore, CT is not sensitive for detecting pathologic alterations in CSF protein. The pathologic alterations are related predominantly to the hemoglobin molecule, not to the iron or protein content. In this study, above a Hct of 27% blood, the mixture was shown to be denser on CT scans than was the normal cortex. Our results are almost the same as those of previous reports (18) and explain why CT often fails to reveal minor leaks; at low Hct levels, the CT values become progressively less than those of normal cortex, and therefore leaks are more difficult to see.

The two primary mechanisms for T1 shortening in intracranial hemorrhages are bound water and paramagnetic effects (19). Bradley and Schmidt

(4), in an *in vitro* study, did not observe the formation of a significant quantity of methemoglobin until several days after the occurrence of SAH. Therefore, the T1 shortening of acute SAH relative to the CSF may reflect the increase in hydration-layer water due to the higher protein content of the bloody CSF (19). In our study, T1 relaxation times for blood were shown to shorten with increasing Hct (ie, increasing protein concentration). Changes in CSF T1 and T2 relaxation times resulting from increases in protein concentration are more conspicuous on FLAIR images than on conventional T1- and T2-weighted spin-echo MR images (20).

The variable MR appearance of intracranial hemorrhages depends on the structure of the hemoglobin and its various oxidation products. In addition, the marked T2 shortening due to the deoxy form of hemoglobin is observed in acute intraparenchymal hemorrhages (21); however, SAH differs from intraparenchymal hemorrhage in that it is mixed with CSF at high oxygen tension. Grossman et al (22, 23) presented *in vitro* data suggesting that the high oxygen tension of CSF imposed restrictions on the generation of paramagnetic deoxyhemoglobin in CSF blood. These investigators proposed that CSF blood was not seen as an area of marked hypointensity because of the lack of deoxyhemoglobin formation from diamagnetic oxyhemoglobin.

Hayman et al (24) reported that the signal intensity on T2-weighted images depends primarily on the state of the RBC hydration, and that sufficient RBC dehydration causes a marked decrease in T2 relaxation time relative to that of the brain parenchyma. Conversely, sufficient RBC overhydration or lysis of RBC causes a marked increase. Therefore, it is possible that RBC overhydration, not dehydration, or RBC lysis causes the lack of marked hypointensity of SAH on T2-weighted images. This can be explained by the bleeding into the CSF space and restricted paramagnetic deoxyhemoglobin generation arising from the high oxygen tension of CSF.

On the FLAIR images, T1 shortening of bloody CSF due to the higher protein content causes an offset in the null of the CSF inversion time, resulting in increased signal intensity. Heavy T2 weighting preferentially suppresses signal intensity from the brain parenchyma compared with bloody CSF (because the T2 relaxation time of some bloody CSF is longer than that of the brain parenchyma), thus allowing the signal intensity from bloody CSF to exceed that of the brain parenchyma. The combination results in improved sensitivity to increases in CSF signal intensity.

Rydberg et al (15) reported the effects of varying the effective TE in turbo-FLAIR imaging. They found that with turbo-FLAIR imaging of subtle lesions, such as multiple sclerosis plaques using a TR of 8000 and inversion time of 2300, optimal lesion contrast could be obtained using a TE of 140 for typical multiple sclerosis plaques or a TE of 160

for more subtle plaques. Melhem et al (20) also showed that FLAIR imaging with high effective TE is more sensitive to elevations in CSF protein. In our study, a longer effective TE, theoretically, will enable detection of bloody CSF with smaller increases in Hct; however, increases in effective TE are limited by image degradation resulting from poor signal-to-noise ratios. The suitable TE may be approximately 160 for the detection of acute SAH.

Screening for SAH with turbo-FLAIR imaging is flow-related. Artifactual CSF hyperintensity may occur with turbo-FLAIR imaging and may be most prominent in the ventricular system and basal cistern (25). Section-selective inversion pulses with broad bandwidth and non-section-selective inversion pulses or cardiac gating are some of the techniques that are used to reduce this artifact (26). In addition, one must also be aware of artifactual CSF hyperintensity related to magnetic field alterations caused by metal (27). Another limitation of FLAIR imaging is its lack of specificity for acute SAH because of any condition that leads to increased CSF protein concentration (20). Singer et al (10) also reported that FLAIR imaging seems to be highly sensitive but nonspecific for acute SAH. Further experience may be needed in diagnosing acute SAH by using FLAIR imaging.

There are a number of major limitations of this *in vitro* study as well as of the previously reported *in vitro* study presented by Chakeres and Bryan (18), including that there was no movement (circulation and pulsation) of the mixtures. There are rapid metabolic changes of blood in the subarachnoid spaces related to hemolysis and WBC phagocytosis. The MR signal intensity changes related to oxygenation, pH, breakdown of the hemoglobin pigments, and clot lysis cannot be simulated in an *in vitro* model (4, 28–30).

Conclusion

In this *in vitro* study, above a Hct of 27% blood, the mixture appears denser on CT scans than is normal for cortical gray matter. On the other hand, at a selected time longer than an effective TE of 120, above a Hct of 22.4% blood, the mixture was more hyperintense than the normal cortical gray matter on turbo-FLAIR images. At selected times longer than an effective TE of 160, above a Hct of 9% blood, the mixture was more hyperintense than the normal cortical gray matter. These results show that a small amount of acute SAH diluted by CSF that is not well shown as a high-attenuation area on CT scans may have a high signal intensity area on FLAIR images. The small amount of acute SAH diluted by CSF is more readily identified with FLAIR imaging than with CT at an appropriate TE.

Acknowledgments

We thank Hideto Toyoshima, BS, for assistance in calculating relaxation times, Hisashi Yoshida, BS, for photographic

assistance, and Yuji Ikeda, BS, and Koichi Mori, BS, for assistance with the MR examinations.

References

1. Leblanc R. **The minor leak preceding subarachnoid hemorrhage.** *J Neurosurg* 1987;66:35-39
2. Okawara S. **Warning signs prior to rupture of an intracranial aneurysm.** *J Neurosurg* 1973;38:575-580
3. Vermeulen M, van Gijn J. **The diagnosis of subarachnoid haemorrhage.** *J Neurol Neurosurg Psychiatry* 1990;53:365-372
4. Bradley WG, Schmidt PG. **Effect of methemoglobin formation on the MR appearance of subarachnoid hemorrhage.** *Radiology* 1985;156:99-103
5. Zimmerman RD, Heier LA, Snow RB, Liu DPC, Kelly AB, Deck MDF. **Acute intracranial hemorrhage: intensity on sequential MR scans at 0.5-T.** *AJR Am J Roentgenol* 1988;150:651-661
6. Atlas SW. **MR Imaging is highly sensitive for acute subarachnoid hemorrhage . . . Not!** *Radiology* 1993;186:319-332
7. Noguchi K, Ogawa T, Inugami A, Toyoshima H, Okudera T, Uemura K. **MR of acute subarachnoid hemorrhage: a preliminary report of fluid-attenuated inversion recovery pulse sequences.** *AJNR Am J Neuroradiol* 1994;15:1940-1943
8. Noguchi K, Ogawa T, Inugami A, et al. **Acute subarachnoid hemorrhage: MR imaging with fluid-attenuated inversion recovery pulse sequences.** *Radiology* 1995;196:773-777
9. Noguchi K, Ogawa T, Seto H, et al. **Subacute and chronic subarachnoid hemorrhage: diagnosis with fluid-attenuated inversion recovery MR imaging.** *Radiology* 1997;203:257-262
10. Singer MB, Atlas SW, Drayer BP. **Subarachnoid space disease: diagnosis with fluid-attenuated inversion recovery MR imaging and comparison with gadolinium-enhanced spin-echo MR imaging-blinded reader study.** *Radiology* 1998;208:417-422
11. Chrysikopoulos H, Papanikolaou N, Pappas J, et al. **Acute subarachnoid haemorrhage: detection with magnetic resonance imaging.** *Br J Radiol* 1996;69:601-609
12. Oka K, Yamamoto M, Nonaka T, Tomonaga M. **The significance of artificial cerebrospinal fluid as perfusate and endoneurosurgery.** *Neurosurgery* 1996;38:733-736
13. Dickinson R, Hall A, Hind A, et al. **Measurement of changes in tissue temperature using MR imaging.** *J Comput Assist Tomogr* 1986;10:468-472
14. Cohen MD, McGuire W, Cory DA, Smith JA. **MR appearance of blood and blood products: an in vitro study.** *AJR Am J Roentgenol* 1986;146:1293-1297
15. Rydberg JN, Riederer SJ, Rydberg CH, Jack CR. **Contrast Optimization of fluid-attenuated inversion recovery (FLAIR) imaging.** *Magn Reson Med* 1995;34:868-877
16. Scotti G, Ethier R, Melancon D, Terbrugge K, Tchang S. **Computed tomography in the evaluation of intracranial aneurysms and subarachnoid hemorrhage.** *Radiology* 1977;123:85-90
17. Norman D, Price D, Boyd D, Fishman R, Newton TH. **Quantitative aspects of computed tomography of the blood and cerebrospinal fluid.** *Radiology* 1977;123:335-338
18. Chakeres DW, Bryan RN. **Acute subarachnoid hemorrhage: in vitro comparison of magnetic resonance and computed tomography.** *AJNR Am J Neuroradiol* 1986;7:223-228
19. Bradley WG. **MR appearance of hemorrhage in the brain.** *Radiology* 1993;189:15-26
20. Melhem ER, Jara H, Eustace S. **Fluid-Attenuated inversion recovery MR imaging: identification of protein concentration thresholds for CSF hyperintensity.** *AJR Am J Roentgenol* 1997;169:859-862
21. Gomori JM, Grossman RI, Goldberg HI, et al. **Intracranial hematoma: imaging by high field MR.** *Radiology* 1985;157:87-93
22. Grossman RI, Kemp SS, Yu IC, et al. **The importance of oxygenation in the appearance of acute subarachnoid hemorrhage on high-field magnetic resonance imaging.** *Acta Radiol* 1986;369[Suppl]:56-58
23. Grossman RI, Gomori JM, Goldberg HI, et al. **MR imaging of hemorrhage conditions of the head and neck.** *RadioGraphics* 1988;8:441-454
24. Hayman LA, Tuber KH, Ford JJ, Bryan RN. **Mechanisms of MR signal alteration by acute intracerebral blood: old concepts and new theories.** *AJNR Am J Neuroradiol* 1991;12:899-907
25. De Coene B, Hajnal JV, Gatehouse P, et al. **MR of the brain using fluid-attenuated inversion recovery (FLAIR) pulse sequences.** *AJNR Am J Neuroradiol* 1992;13:1555-1564
26. Hashemi RH, Bradley WG, Chen DY, et al. **Suspected multiple sclerosis: MR imaging with a thin-section fast FLAIR pulse sequence.** *Radiology* 1995;196:505-510
27. Adams JG, Melhem ER. **Clinical usefulness of T2-weighted fluid-attenuated inversion recovery MR imaging of the CNS.** *AJR Am J Roentgenol* 1999;172:529-536
28. Koivula A, Suominen K, Timonen T, Kiviniitty K. **The spin-lattice relaxation time in the blood of healthy subjects and patients with malignant blood disease.** *Phys Med Biol* 1982;27:937-947
29. Thulborn KR, Waterton JC, Matthews PM, Radda GK. **Oxygenation dependent of the transverse relaxation time of water protons in whole blood at high field.** *Biochim Biophys Acta* 1982;714:265-270
30. Morariu VV, Pop VI, Popescu O, Benga G. **Effects of temperature and pH on the water exchange through erythrocyte membrane: nuclear magnetic resonance studies.** *J Membr Biol* 1981;62:1-5